
Modeling the Temporal-Pulse-Shape Dynamics of an Actively Stabilized Regenerative Amplifier for OMEGA Pulse-Shaping Applications

Advances in laser-fusion technology indicate that the temporal profile of the laser pulse applied to laser-fusion targets is important for improving the performance of these targets.¹ The OMEGA laser is a 60-beam laser-fusion system capable of producing a total of 30 kJ of ultraviolet (351-nm) energy on target, where the temporal profile of the optical pulse applied to a laser-fusion target can be specified in advance. This is accomplished by a pulse-shaping system that produces an optical pulse with a specific temporal pulse shape at the nanojoule energy level.² This pulse seeds an actively stabilized Nd:YLF regenerative amplifier³ (regen) followed by and wavelength matched (1053 nm) to a series of Nd:glass amplifiers. The beams are then frequency tripled to the third harmonic using KDP nonlinear crystals. To achieve the desired on-target optical pulse shape, the temporal dynamics of the entire OMEGA laser system must be accurately modeled to determine the specific temporal profile of the seed pulse required from the pulse-shaping system at the beginning of the laser. The temporal profile of this low-energy seed pulse, when amplified and frequency tripled by the laser system, will then compensate for the temporal distortions caused by gain saturation in the regen and amplifiers and by the tripling process, and will produce the desired pulse shape on target.

To determine the required temporal profile of the optical pulse at the beginning of the system, all sources of temporal distortions in the system must be understood and compensated for. The temporal distortion due to the frequency-tripling process is modeled with a time-dependent simulation of the appropriate nonlinear equations for this process.⁴ The temporal-pulse distortions in the system's Nd:glass amplifiers are easily modeled with our beam code *RAINBOW*. Modeling the actively stabilized Nd:YLF regen at the beginning of the system is the topic of this article. With the regen model described here, OMEGA's temporal dynamics can now be completely modeled. Pulse distortions in the system can be easily compensated for by proper choice of the seed temporal profile determined from the overall model.

The gain of the OMEGA system from the pulse-shaping modulator to the target is approximately 10^{14} ; a gain of 10^7 in the actively stabilized regen is included in this overall gain. Modeling the actively stabilized regen is complicated by many factors. The regen must be treated as a multipass amplifier, the last few passes of which experience significant gain saturation in the Nd:YLF laser rod. The lifetime of the lower-laser-level manifold in Nd:YLF has been measured to be 21 ns,⁵ and the round-trip time in the cavity is 26 ns. A Frantz-Nodvik-type solution⁶ for the gain in the Nd:YLF medium cannot account for this finite lower-laser-level lifetime and, hence, is inappropriate; the rate equations must be used to describe the single-pass gain in the Nd:YLF medium. Finally, the regen incorporates a feedback mechanism that measures the circulating pulse energy each round-trip.³ When the circulating pulse energy exceeds a threshold ($\sim 25 \mu\text{J}$), a feedback mechanism is activated. The feedback mechanism introduces appropriate losses into the cavity each round-trip in order to stabilize the circulating pulse energy to a fixed but low-energy level. During this prelude stabilization phase the regen is operating with a net gain (round-trip gain/loss) approximately equal to unity and establishes a constant and stable pulse-energy output from the regen. After this prelude stabilization is achieved, the laser can be *Q*-switched by eliminating the feedback losses from the cavity. The regen will then emit a *Q*-switched envelope of pulses. The pulse at the peak of the *Q*-switched envelope is switched out and sent to the OMEGA amplifiers. This stabilized regen produces pulses with a long-term shot-to-shot energy stability of approximately 0.2%, despite the fluctuations introduced by the flash-lamp pumping, and is insensitive to injected-pulse energy variations of more than two orders of magnitude.³

The regen is modeled by numerical integration of the rate equations and careful consideration of the regen dynamics. The regen model described here includes gain saturation in the Nd:YLF laser rod, intracavity losses, lower-laser-level lifetimes, and the active losses introduced by the stabilizer-feed-

back circuit. Careful measurements of the input and output shaped optical pulses from the regen have been made and will be discussed. The calculations on this regen agree well with the measured output of the regen and serve as a model for this important OMEGA component. With this regen model, the entire temporal-pulse-shaping dynamics of OMEGA can now be modeled from the pulse-shaping system to the final on-target pulse shape. This modeling provides us with the capability to accurately produce any desired temporally shaped optical pulse on target for laser-fusion experiments.

Rate Equations

OMEGA's pulse-shaping system produces a shaped optical pulse that is injected into the actively stabilized regenerative amplifier. The output-pulse shape of the regen is determined by gain saturation in the active medium and by the cavity dynamics. The regen model consists of injecting a temporally shaped pulse into the cavity and calculating the new shape after every pass through the cavity. The effect on the pulse shape due to each component is treated separately in the calculation. In this section we discuss the temporal distortion due to a single pass through the gain medium and in the next section incorporate this into the calculation of the overall regen dynamics.

Gain saturation due to a single pass through a gain medium is calculated by solving the laser rate equations⁷

$$\begin{aligned} & \frac{\partial \varphi(z,t)}{\partial t} + \frac{c}{n} \frac{\partial \varphi(z,t)}{\partial z} \\ &= \frac{c \sigma \varphi(z,t)}{n} [f_2 N_2(z,t) - f_1 N_1(z,t)], \end{aligned} \quad (1a)$$

$$\begin{aligned} \frac{\partial N_1(z,t)}{\partial t} &= \frac{c \sigma \varphi(z,t)}{n} [f_2 N_2(z,t) - f_1 N_1(z,t)] \\ &+ \frac{N_2(z,t)}{\tau_{21}} - \frac{N_1(z,t)}{\tau_{10}}, \end{aligned} \quad (1b)$$

$$\begin{aligned} \frac{\partial N_2(z,t)}{\partial t} &= -\frac{c \sigma \varphi(z,t)}{n} \\ &\times [f_2 N_2(z,t) - f_1 N_1(z,t)] - \frac{N_2(z,t)}{\tau_{21}}, \end{aligned} \quad (1c)$$

which describe the evolution of the cavity photon flux φ , the atomic population N_1 of the lower laser manifold, and the atomic population N_2 of the upper laser manifold. These rate equations explicitly account for the lifetimes of these upper

and lower laser manifolds. In these equations c is the speed of light in vacuum; n is the index of refraction of the gain medium; σ is the stimulated emission cross section ($1.2 \times 10^{-19} \text{ cm}^2$); and $\tau_{i,j}$ is the relaxation time of the transition from manifold i to manifold j (here, level 0 represents the ground state). The upper laser manifold N_2 consists of two sublevels labeled with energies $E_{2,n}$ ($n = 1, 2$), and the lower laser manifold N_1 consists of six sublevels labeled with energies $E_{1,m}$ ($m = 1$ to 6), two of which are degenerate in energy (sublevels 2 and 3) as shown in Fig. 69.19. The stimulated emission terms in the rate equations [Eqs. (1)] (first terms on the right side in each equation) involve transitions between the sublevels E_{21} and E_{12} as shown in Fig. 69.19; hence, the thermal occupation $f_i N_i$ of these laser-active sublevels is used in these terms. The thermal occupation of these sublevels is calculated by

$$f_1 N_1 = \frac{e^{-E_{12}/kT} N_1}{\sum_{m=1}^{m=6} e^{-E_{1m}/kT}} = 0.207 N_1 \quad (2a)$$

and

$$f_2 N_2 = \frac{e^{-E_{21}/kT} N_2}{e^{-E_{21}/kT} + e^{-E_{22}/kT}} = 0.570 N_2, \quad (2b)$$

where $E_{i,j}$ is the energy of level i sublevel j relative to the lowest

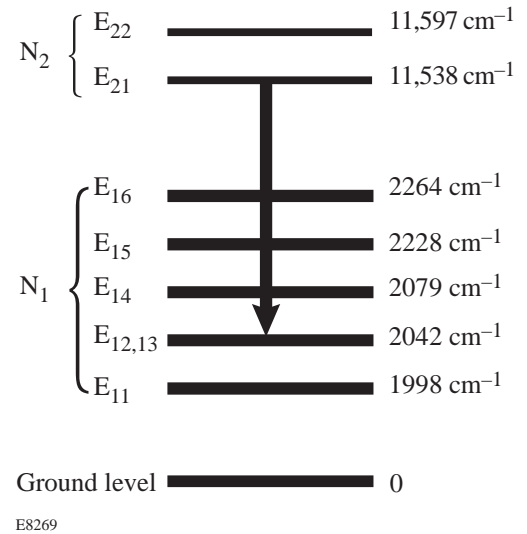


Figure 69.19 The energy levels involved in the 1.053- μm -Nd:YLF laser transition. The arrow shows the laser transition between sublevels within the manifolds shown.

energy level in the manifold, k is the Boltzman constant, and T is the temperature (assumed to be room temperature).

The rate equations [Eqs. (1)] can be solved numerically. We transform these equations along their characteristics in the time-distance plane with the transformation equations

$$x \rightarrow z + \frac{ct}{n} \quad \tau \rightarrow t - \frac{nz}{c}. \quad (3)$$

If we use the chain rule and the substitution

$$\Delta N = \frac{\sigma\phi(x)}{2} [f_2 N_2(z, t) - f_1 N_1(z, t)] dx \quad (4)$$

with $cdt/n = dz = dx/\sqrt{2}$, we get the set of finite-difference equations

$$d\phi = \Delta N, \quad (5a)$$

$$dN_1 = \sqrt{2} \Delta N + \frac{N_2}{\tau_{21}} dt - \frac{N_1}{\tau_{10}} dt, \quad (5b)$$

$$dN_2 = -\sqrt{2} \Delta N - \frac{N_2}{\tau_{21}} dt \quad (5c)$$

for the transformed rate equations. Here we have transformed Eq. (1a) using the transformation equations [Eqs. (3)], and we have left Eqs. (1b) and (1c) untransformed since the photon flux evolves in both space and time, whereas the populations evolve in time only. These equations can be solved numerically given appropriate boundary conditions.

In the model, the photon flux is specified at the entrance face of the laser rod and is given by the temporal profile of the pulse entering the rod. The initial upper-laser-level population is determined from measurements of the laser rod small-signal gain, and for simplicity the initial lower-laser-level population is assumed to be zero. With these boundary conditions, Eqs. (5) can be numerically integrated to yield the photon flux at any time and for any position in the laser rod. Of interest for our calculations is the output-pulse shape specified at the

output face of the laser rod. These equations with these boundary conditions, along with the regen dynamics discussed below, have been solved numerically, and the results are presented below.

Regenerative Amplifier Model

Modeling the regen consists of injecting a pulse with a given pulse shape and energy into the regen and calculating the new pulse shape and energy after each round-trip through the cavity. A single round-trip through the regenerative amplifier is depicted in Fig. 69.20. The pulse first experiences gain through the laser rod followed by propagation to the output-coupling mirror and back. The pulse then experiences gain again followed by propagation to the end mirror and back. Losses due to the output-coupling mirror and the feedback stabilizer (discussed below) are included in the calculation. During propagation of the pulse in the cavity, the upper- and lower-laser-level manifolds are allowed to decay with their respective lifetimes. This calculation for a single pass through the cavity gives the output-pulse shape and energy, given the input-pulse shape and energy for the pass. The output pulse for each pass is used as the input pulse for the next pass through the cavity, and the procedure is repeated for a given number of round-trips through the cavity.

The loss due to the feedback stabilizer depends on several factors. The cavity incorporates two Pockels cells, one of which is feedback controlled. Specific voltages are applied to all four electrodes of the two Pockels cells at specific times.³ During the beginning of the flash-lamp cycle, high losses are introduced into the cavity to allow the gain to build up in the rod. At the peak of the gain, a pulse is injected into the cavity at time t_1 , and all losses are removed from the cavity (with the exception of the static losses here assumed to be 55% in our laser, which includes the 50% output coupler loss) allowing the circulating-pulse energy to increase. The applied voltages after time t_1 are shown schematically in Fig. 69.21(a) (however, not to scale). When the circulating-pulse energy reaches a threshold value (adjusted to $\sim 25 \mu\text{J}$), the feedback stabilizer is activated. At this time (t_2) a dc voltage V_{dc} is applied to one electrode of the first Pockels cell, which introduces a dc loss into the cavity. Simultaneously, a modulated feedback-con-

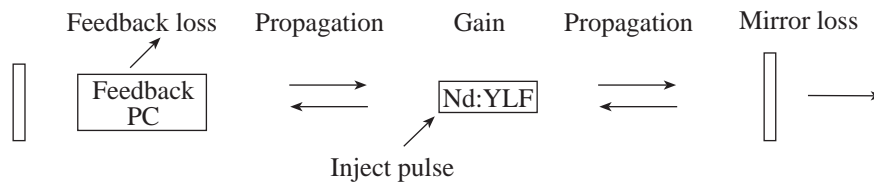
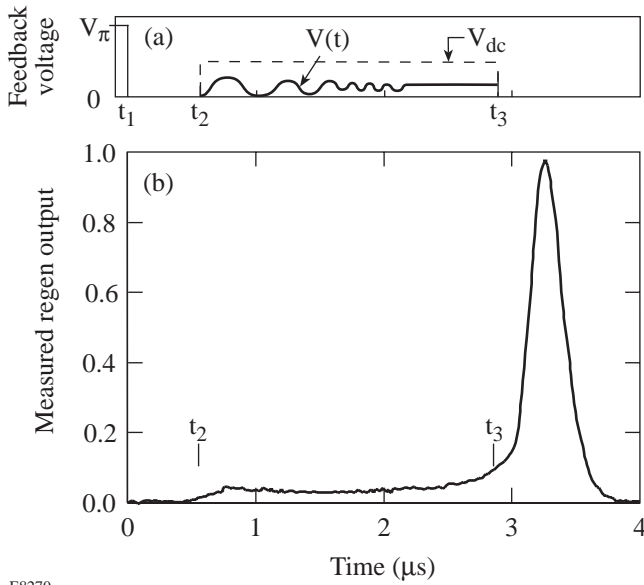


Figure 69.20
The regen model calculates the pulse shape and energy after a round-trip in the cavity, then iterates for many round-trips. The calculation includes the effects of gain saturation, propagation, and static and feedback losses.

E8313



E8270

Figure 69.21
 Regen temporal dynamics showing (a) feedback-controlled Pockels cell voltages (not to scale), and (b) measured regen-output envelope filtered to remove individual pulses in the train.

trolled voltage $V(t)$ is applied to an electrode of the feedback-controlled Pockels cell, which introduces a feedback-controlled modulated loss in the cavity. The function of the feedback-controlled modulated loss is to stabilize the circulating pulse energy to a specified constant low value. If the pulse energy falls below (above) this energy, loss is removed (added) to maintain the specified output-pulse energy. Specially designed circuitry for this modulated feedback-controlled voltage³ eliminates pulse-shape distortions caused by fast feedback-voltage changes during pulse propagation through the Pockels cell, as in the previous design.⁸ This ensures that pulse-shape distortions in the regen are due mainly to gain saturation. Finally, after the output-pulse energy is stabilized by the feedback mechanism during this prelude phase, the laser is Q -switched, at which time (t_3) all feedback loss is removed and a Q -switched pulse envelope is allowed to build up. (During this time an adjustable low-level dc loss is left in the cavity to control the final output-pulse energy; however, this loss is not included in the model.) The measured output-pulse train envelope from the regen is shown in Fig. 69.21(b).

The voltage applied to the feedback-controlled Pockels cell during the prelude stabilization is modulated every round-trip so that the Pockels cell transmission is given by

$$T = \cos^2\left(\frac{\pi}{2} \frac{V(t)}{V_\pi}\right), \quad (6)$$

where $V(t)$ is the instantaneous value of the modulated voltage difference between the electrodes and V_π is the quarter-wave voltage of the Pockels cell. The modulated voltage for a particular pass when the feedback circuitry is active is modeled by

$$V_{i+1} = [V_i + \Delta V_i] e^{-\tau_{rt}/\tau_{fb}}, \quad (7)$$

where V_i is the value of the modulated voltage at the beginning of the pass, ΔV_i is the increase in voltage due to the feedback circuitry, and V_{i+1} is the value of the modulated voltage after the pass. The change in voltage ΔV_i is given by

$$\Delta V_i = \text{pulse energy (J)} \times \text{feedback gain (V/J)}, \quad (8)$$

where the feedback gain is determined by the feedback circuitry. In Eq. (7), the final voltage is allowed to decay every round-trip (round-trip time $\tau_{rt} = 26$ ns) with the exponentially decreasing feedback decay time $\tau_{fb} = 35$ ns. When the laser is Q -switched at time t_3 , all feedback loss is removed from the cavity allowing the free buildup of the Q -switched pulse train.

The above model describes how to calculate the output-pulse shape from the regen given the input-pulse shape. Often it is necessary to calculate the inverse, that is, calculate the required input-pulse shape to the regen that will produce a desired output-pulse shape. A good approximation for this input-pulse shape can be gotten from the output-pulse shape with a simple procedure. A transfer function for the regen can be calculated by using the desired regen-output-pulse shape $[I^{\text{out}}(t)]$ as input to the calculation to obtain a new output-pulse shape [e.g., $I^{\text{new}}(t)$]. The transfer function $T(t)$ for the regen is obtained by dividing these two functions to get

$$T(t) = \frac{I^{\text{new}}(t)}{I^{\text{out}}(t)}. \quad (9)$$

The required input-pulse shape $[I^{\text{in}}(t)]$ can now be calculated with this transfer function and is given by

$$I^{\text{in}}(t) = \frac{I^{\text{out}}(t)}{T(t)}. \quad (10)$$

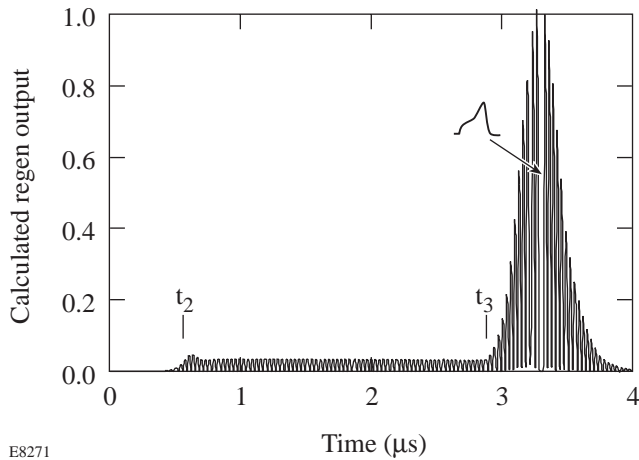
This simple procedure is used to obtain the required regen-input-pulse shape that will produce the desired regen-output-pulse shape. More importantly, this procedure is useful in producing the desired OMEGA on-target pulse shape.

Experiments

The regen in OMEGA uses a Nd:YLF laser rod pumped to a single-pass, small-signal gain of approximately 2.9. The laser uses a 50% reflecting output coupler, the cavity-round-trip time is 26 ns, and the laser operates at 5 Hz. Typical output energies of the pulse switched out at the peak of the *Q*-switched envelope are approximately 1.0 mJ.

The measured output-pulse train from the regen is shown in Fig. 69.21(b). The output has been filtered to show only the envelope of the pulse-train output from the regen. It can be seen that the feedback is activated at time t_2 approximately 600 ns after the pulse is injected into the cavity at time $t_1 = 0$. At $t_3 = 2.9 \mu\text{s}$, the laser is *Q*-switched and a pulse train builds up and decays as the gain is depleted.

Figure 69.22 shows the calculated-output-pulse train from the regen for the above case. Individual pulses within the train are shown. The calculation is based on the model described above with typical values for the regen parameters. Note the good agreement between the measured-output-pulse train in Fig. 69.21(b) and the predictions shown in Fig. 69.22.



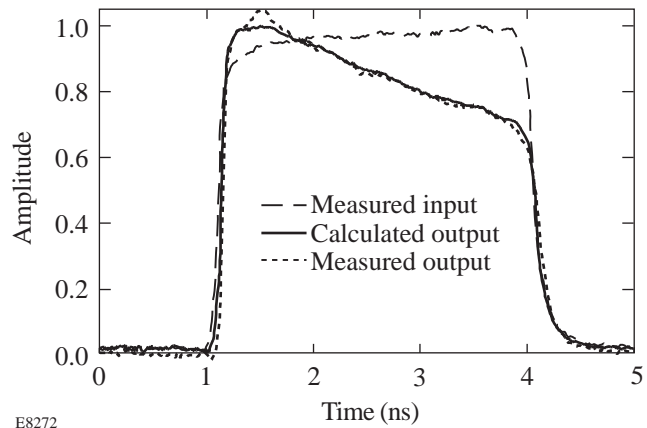
E8271

Figure 69.22
Calculated regen-output envelope corresponding to the case measured in Fig. 69.21(b). Individual pulses are shown.

Figure 69.23 shows regen input/output-pulse shapes for a square pulse injected into the regen. The output-pulse shape is the pulse that is switched out at the peak of the *Q*-switched envelope. The input square pulse (curve plotted with long dashed lines) and measured-regen-output pulse (curve plotted with short dashed lines) are shown in Fig. 69.23, along with the calculated-output-pulse shape (curve plotted with solid line) obtained with the above numerical method using the measured-square-pulse shape as input to the calculation. The regen parameters used in the calculation correspond to the measured regen parameters with slight adjustments to obtain good agreement with the data. By adjusting the regen parameters in this way, the model is calibrated to the data. Once this calibration procedure is performed, the parameters in the model are left unchanged and other shaped pulses can be calculated and compared to measurements.

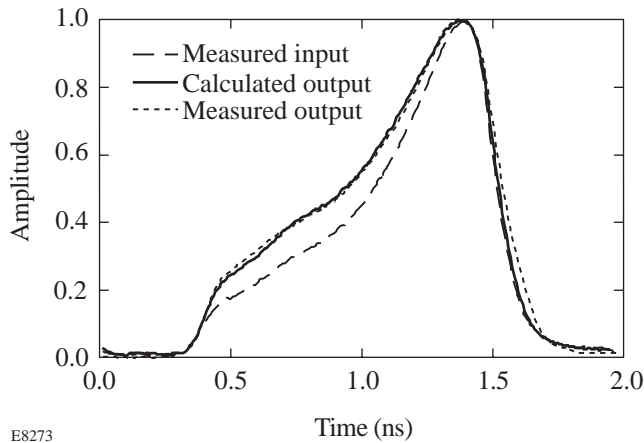
Figure 69.24 shows the same information as Fig. 69.23, but for a shaped optical pulse injected into the regen. The regen parameters were identical to those used for the calculation in Fig. 69.23. This pulse shape, when injected into OMEGA, will produce a square pulse shape at 351-nm wavelength at the output of OMEGA.

In summary, we have modeled the temporal evolution of a shaped optical pulse injected into our feedback-stabilized regen to a high degree of accuracy. We have solved the rate



E8272

Figure 69.23
Square-pulse distortion from the regen showing the input-pulse shape (long dashed lines), the measured-output-pulse shape (short dashed lines), and the calculated-output-pulse shape (solid line).



E8273

Figure 69.24

Shaped pulse from the regen showing the input-pulse shape (long dashed lines), the measured-output-pulse shape (short dashed lines), and the calculated-output-pulse shape (solid line).

equations including upper- and lower-laser-level lifetimes explicitly. We provide a prescription for determining the injection-pulse shape required to produce a given output-pulse shape from this regen. Finally, with this model of the regen, the entire OMEGA laser system can be modeled, and on-target pulse shapes can be specified in advance by OMEGA users.

ACKNOWLEDGMENT

This work was supported by the U.S. Department of Energy Office of Inertial Confinement Fusion under Cooperative Agreement No. DE-FC03-92SF19460, the University of Rochester, and the New York State Energy Research and Development Authority. The support of DOE does not constitute an endorsement by DOE of the views expressed in this article.

REFERENCES

1. J. D. Lindl, *Phys. Plasmas* **2**, 3933 (1995).
2. A. Okishev, M. D. Skeldon, S. A. Letzring, W. R. Donaldson, A. Babushkin, and W. Seka, in *Superintense Laser Fields*, edited by A. A. Andreev and V. M. Gordienko (SPIE, Bellingham, WA, 1996), Vol. 2770, pp. 10–17.
3. A. Babushkin, W. Bittle, S. A. Letzring, A. Okishev, M. D. Skeldon, and W. Seka, “Stable, Reproducible, and Externally Synchronizable Regenerative Amplifier for Shaped Optical Pulses for the OMEGA Laser System,” to be presented at Advanced Solid-State Lasers, Orlando, FL, 27–29 January 1997, paper ME9.
4. R. S. Craxton, *IEEE J. Quantum Electron.* **QE-17**, 1771 (1981).
5. J. D. Zuegel and W. Seka, *IEEE J. Quantum Electron.* **31**, 1742 (1995).
6. L. M. Frantz and J. S. Nodvik, *J. Appl. Phys.* **34**, 2346 (1963).
7. A. E. Siegman, *Lasers* (University Science Books, Mill Valley, CA, 1986).
8. A. Okishev, M. D. Skeldon, S. A. Letzring, W. Seka, and I. Will, in *OSA Proceedings on Advanced Solid-State Lasers*, edited by B. H. T. Chai and S. A. Payne (Optical Society of America, Washington, DC, 1995), Vol. 24, pp. 274–276.